

Calculation of the electron mobility and spin lifetime enhancement by strain in thin silicon films

D. Osintsev^{1,2}, V. Sverdlov¹ and S. Selberherr¹

¹ Institute for Microelectronics, TU Wien, Gußhausstraße 27–29, A–1040 Wien, Austria

² Volgograd State Technical University, Lenin Avenue 28, 400131 Volgograd, Russia

Abstract. Spintronics attracts much attention because of the potential to build novel spin-based devices which are superior to nowadays charge-based microelectronic devices. Silicon, the main element of microelectronics, is promising for spin-driven applications. Understanding the details of the spin propagation in silicon structures is a key for building novel spin-based nanoelectronic devices. We investigate the surface roughness-limited electron mobility and spin relaxation in a silicon spin field-effect transistor. Shear strain dramatically influences the spin relaxation, which opens a new opportunity to boost spin lifetime in a silicon spin field-effect transistor.

Introduction

Spintronics is the rapidly developing and promising technology exploiting spin properties of electrons. A number of potential spintronic devices has been proposed [1–3]. Since silicon is the basic material used for manufacturing modern MOSFETs, developing silicon-based nanoelectronic devices utilizing spin properties is promising. Silicon is an ideal material for spintronic applications, because it is composed of nuclei with predominantly zero spin and is characterized by small spin-orbit coupling. Both factors favour a small spin relaxation. However, large spin relaxation rates in gated silicon structures have been experimentally observed. Understanding the details of the spin propagation in modern ultra-scaled silicon MOSFETs is urgently needed [4].

1. Model

We study electron scattering and spin relaxation processes dominated by surface roughness. The subband energies and wave functions were obtained from a $\mathbf{k} \times \mathbf{p}$ Hamiltonian [5, 6] generalized to include the spin degree of freedom [4, 7]. The Hamiltonian is written in the vicinity of the X -point along the k_z -axis in the Brillouin zone and includes the two relevant valleys of the conduction band [8]. After a unitary basis transformation it is written as

$$H = \begin{bmatrix} H_1 & H_3 \\ H_3 & H_2 \end{bmatrix}, \quad (1)$$

with

$$H_{1,2} = \left[\frac{\hbar^2 k_z^2}{2m_l} + \frac{\hbar^2 (k_x^2 + k_y^2)}{2m_t} + U(z) + (-1)^j \delta \right] I, \quad (2)$$

$$H_3 = \begin{bmatrix} \frac{\hbar^2 k_0 k_z}{m_l} & 0 \\ 0 & \frac{\hbar^2 k_0 k_z}{m_l} \end{bmatrix}. \quad (3)$$

Here I is the identity 2×2 matrix, $U(z)$ is the confinement potential, $\delta = \sqrt{(D\varepsilon_{xy} - \hbar^2 k_x k_y / M)^2 + \Delta_{so}^2 (k_x^2 + k_y^2)}$, ε_{xy} denotes the shear strain component, $M^{-1} \approx m_t^{-1} - m_0^{-1}$, $D = 14$ eV is the shear strain deformation potential, and $\Delta_{so} = 1.27 m$ eV nm, m_t and m_l are the transversal and the longitudinal silicon effective masses, $k_0 = 0.15 \times 2\pi/a$ is

the position of the valley minimum relative to the X -point in unstrained silicon.

The surface roughness scattering matrix element between the subbands is taken to be proportional to the product of the subband wave function derivatives at the interface [9].

Scattering and spin relaxation rates are calculated in the following way [7, 9]

$$\frac{1}{\tau_{SR}} = \frac{\int \frac{1}{\tau_{SR}(\mathbf{K}_1)} f(E) (1 - f(E)) d\mathbf{K}_1}{\int f(E) d\mathbf{K}_1}, \quad (4)$$

$$f(E) = \frac{1}{1 + \exp\left[\frac{E - E_F}{k_B T}\right]}, \quad (5)$$

$$\int d\mathbf{K}_1 = \int_0^{2\pi} \int_0^\infty \frac{|\mathbf{K}_1(\varphi, E)|}{\left|\frac{\partial E(\mathbf{K}_1)}{\partial \mathbf{K}_1}\right|} d\varphi dE, \quad (6)$$

$$\begin{aligned} \frac{1}{\tau_{SR}(\mathbf{K}_1)} &= \frac{4\pi}{\hbar} \sum_{i,j=1,2} \int_0^{2\pi} \pi \Delta^2 L^2 \frac{1}{\varepsilon_{ij}(\mathbf{K}_2 - \mathbf{K}_1)} \\ &\times \frac{\hbar^4}{4m_l^2} \left[\frac{d\Psi_{i\mathbf{K}_1}^*}{dz} \frac{d\Psi_{j\mathbf{K}_2}}{dz} \right]_{z=\pm t/2}^2 \\ &\times \exp\left[\frac{-(\mathbf{K}_2 - \mathbf{K}_1)^2 L^2}{4} \right] \frac{|\mathbf{K}_2(\varphi, E)|}{\left|\frac{\partial E(\mathbf{K}_2)}{\partial \mathbf{K}_2}\right|} \frac{1}{4\pi^2} d\varphi, \end{aligned} \quad (7)$$

where, E is the electron energy, $\mathbf{K}_{1,2}$ is the in-plane wave vector, k_B is the Boltzmann constant, T is the temperature, E_F is the Fermi energy, ε_{ij} is the dielectric permittivity, L is the autocorrelation length, Δ is the mean square value of surface roughness fluctuations.

If the dependence of the wave function derivatives on the wave vector can be neglected [9], the relaxation rate is written as

$$\begin{aligned} \frac{1}{\tau_{SR}^{\text{th}}(\mathbf{K}_1)} &= \frac{2\pi \Delta^2 L^2}{\hbar} \sum_{i,j=1,2} \frac{\hbar^4}{4m_l^2} \left[\frac{d\Psi_{i\mathbf{K} \rightarrow 0}^*}{dz} \frac{d\Psi_{j\mathbf{K} \rightarrow 0}}{dz} \right]_{z=\pm t/2}^2 \\ &\times \exp\left[\frac{-(\mathbf{K}_2^2 + \mathbf{K}_1^2) L^2}{4} \right] \frac{m_t}{2\pi \hbar^2} 2\pi I_0(y), \end{aligned} \quad (8)$$

where I_0 is the modified Bessel function of the first kind and $y = -L^2 K_2 K_1 / 2$.

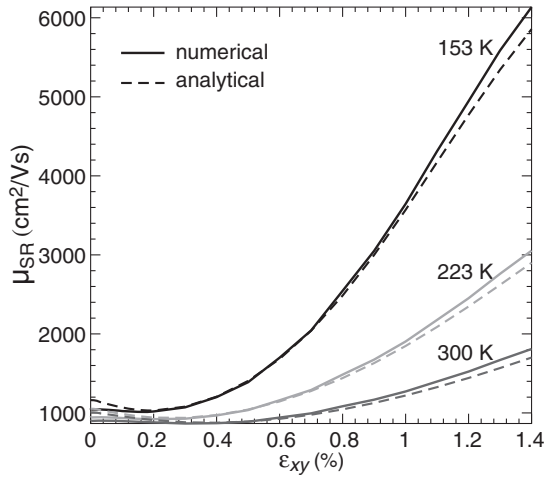


Fig. 1. Dependence of the surface roughness limited mobility on shear strain for different temperatures for an electron concentration 10^{12} cm^{-2} . The numerical and the analytical approaches are compared.

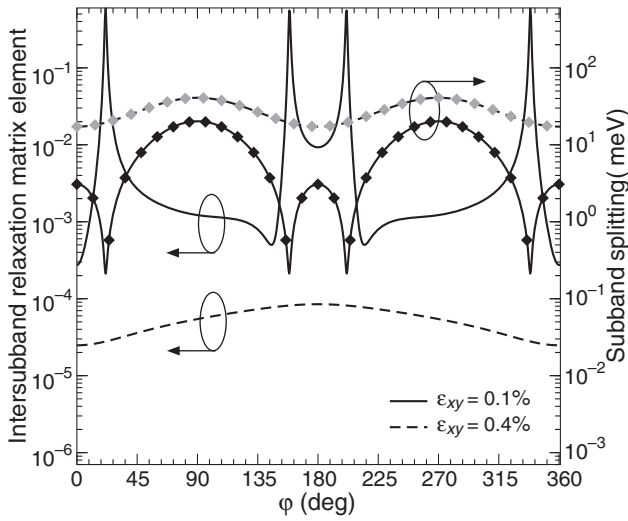


Fig. 2. Intersubband relaxation matrix elements normalized to the intrasubband scattering matrix elements with the lowest electron subband splitting as a function of the angle between the incident and the outgoing wave for $k_x = 0.25 \text{ nm}^{-1}$ and $k_y = 0.25 \text{ nm}^{-1}$.

2. Results and discussion

The simulations were performed for the film thickness 2.48 nm. Fig. 1 shows the surface roughness limited mobility calculated for different temperatures as a function of shear strain. The two curves were computed by using (7) and (8), respectively. While shear strain increases, the discrepancy between the two curves becomes more pronounced, however, even for the shear strain value 1.5% the results are close. Therefore, the standard approximation of ignoring the wave vector dependences in the surface roughness scattering matrix elements (8) is a good approximation for calculating mobilities as demonstrated at different temperature and shear strain values.

Fig. 2 shows the spin relaxation matrix elements due to intersubband transitions normalized to the intrasubband scattering matrix elements at zero strain together with the lowest subbands splitting as a function of the angle between the incident and outgoing wave. For the shear strain value 0.1% the subband splitting shows a strong reduction at the angle val-

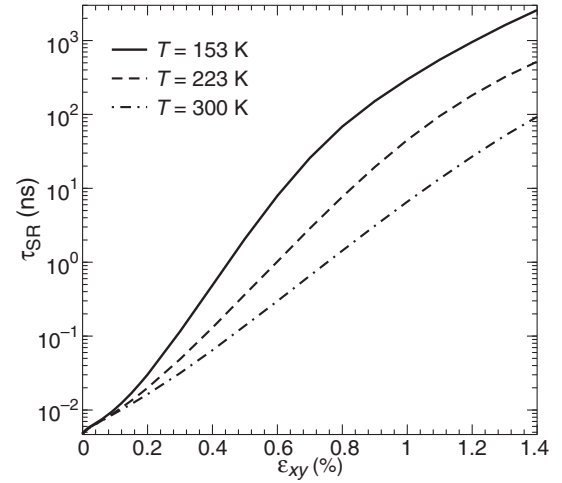


Fig. 3. Dependence of the spin lifetime on tensile shear strain for an electron concentration 10^{12} cm^{-2} , for different temperatures.

ues 20° , 159° , 201° , and 340° . At the same angles the value of the intersubband spin relaxation matrix elements increases. From the Hamiltonian (1) it follows that the sharp minima on the subband splitting are due to the minima of δ . For a fixed shear strain value the minimum of δ is achieved at the value of the wave vector at which the term $D\varepsilon_{xy} - \hbar^2 k_x k_y / M$ vanishes. This is why for larger strain the subband splitting does not display any sharp minima: the shear strain value 0.4% is big enough to prevent zero values of the $D\varepsilon_{xy} - \hbar^2 k_x k_y / M$ term to appear. Thus, the subband splitting smoothly oscillates and no sharp peaks of the intersubband matrix elements are observed, because shear strain pushes regions of the strong spin relaxation to higher energies.

Contrary to the scattering matrix elements, the spin relaxation matrix elements strongly depend on the wave vectors (Fig. 2). Thus, the relaxation time can only be determined by evaluating the integrals (4–7). Spin lifetime enhancement for different values of temperature is shown in Fig. 3. It shows that stress used to enhance mobility can also be used to boost spin lifetime substantially.

Acknowledgements

This work is supported by the European Research Council through the grant #247056 MOSILSPIN. The computational results have been achieved in part using the Vienna Scientific Cluster (VSC).

References

- [1] J. Sinova, I. Zutic, *Nature Materials* **11**, 368 (2012).
- [2] S. Sugahara and J. Nita, *Proc. IEEE* **98**, 2124 (2010).
- [3] D.D. Awschalom and M.E. Flatte, *Nature Physics* **3**, 153 (2007).
- [4] Y. Song, H. Dery, *Physical Review B* **86**, 085201 (2012).
- [5] G.L. Bir, G.E. Pikus, *Symmetry and strain-induced effects in semiconductors*, (J. Wiley&Sons), 1974.
- [6] V. Sverdlov, *Strain-induced effects in advanced MOSFETs*, (Springer), 2011.
- [7] P. Li, H. Dery, *Physical Review Letters* **107**, 107203 (2011).
- [8] D. Osintsev *et al*, *Proc. EUROSOI (Paris, France, 2013)*.
- [9] M.V. Fischetti *et al*, *J. Appl. Phys.* **94**, 1079 (2003).